Comparison of specular gloss values from a spectrally resolved five-axis goniometer and a reference goniophotometer

Renée Charrière*[1,2] *and Maria Nadal*[1] *and Clarence Zarobila*[1] *;* [1] *National Institute of Standards and Technology; Gaithersburg, MD, United States;* [2] *Ecole Nationale Supérieure des Mines de Saint-Etienne, SMS EMSE, CNRS UMR5307, Laboratoire Georges Friedel; Saint-Etienne, France

Abstract

The present work consists in developing a procedure which will allow comparison of gloss values obtained from angularly and spectrally resolved Bidirectional Reflectance Distribution Function (BRDF) measurements and gloss values measured with a national reference goniophotometer. The gloss measurements will be performed on the Reference Goniophotometer for Specular Gloss Calibration available at the Sensor Science Division of the National Institute of Standards and Technology (NIST), whereas the BRDF measurements will be conducted on the Five-Axis Goniometer for Color & Appearance also available at the same division of NIST.

Introduction

The appearance of a product is important for many industries, for example automotive, cosmetics, paper, printing, packaging, coatings, plastics, steel industries, etc., as this is frequently one of the most critical parameters affecting customer decision. Gloss is the second most relevant visual attribute of a surface, second to color. While the perceived color of an object originates from the wavelength distribution of the reflected light, gloss originates from its angular distribution.

A specular glossmeter measures the flux reflected from a specimen in comparison to the flux reflected from a standard under the same standardized measurement conditions. The theoretical primary standard is specified to be a perfect polished material with refractive index of 1.567 at 589.3 nm [1]. In 1939, ASTM adopted the 60° geometry in a standard method, i.e., ASTM method D523 [2]. Two additional measurement procedures were incorporated into ASTM D523 in 1951, with the addition of a 20° geometry test method for the evaluation of high gloss finishes and an 85° geometry test method for the evaluation of low gloss surfaces. Although specular glossmeters have been used in industry for decades, their limited capabilities have been recognized for a long time. The current specular gloss measurement standards fail to distinguish between type of materials or degree of specular gloss [3]. For example, Vienot & Obein compared the gloss of a piece of tire and of a black inked paper [4]. Though both samples reflected almost the same level of lux and have similar specular gloss values, the difference in visual gloss was obvious and all the observers were able not only to correctly rank the gloss, but also to identify the material of which the sample was made of. A study of the angular distribution of the reflected light revealed that the shape of the specular peak was very different between the two samples and suggested that the visual system extracts information not only from the magnitude of the peak but also from the shape of the peak.

Two facilities available at the Sensor Science Division of the National Institute for Standards and Technology (NIST) were used in this work. These facilities are the Five-Axis Goniometer for Color & Appearance [5] and the Reference Goniophotometer for Specular Gloss Calibration [6]. The Five-Axis Goniometer is currently used to measure the Bidirectional Reflectance Distribution Function (BRDF) of gonio-apparent materials, that is, materials that change their appearance as a function of illumination and viewing directions. The Reference Goniophotometer for Specular Gloss Calibration is an aging facility that provides the calibration of specular gloss standards at the specular geometries of 20°, 60° and 85°. The aim pursued here is to perform specular gloss measurements on the Five-Axis Goniometer. This will first allow decommissioning of the present gloss facility and eliminate the need for its upgrade and maintenance. This will also allow to perform angular resolved gloss measurements, which will give us the opportunity for new characterization features of glossy samples.

Definition of gloss

The specular gloss $G_{sple}(\theta_0)$ of a sample, illuminated with light around the direction θ_0 from the normal of the sample surface is defined by :

$$G_{sple}(\theta_0) = G_{p-std}(\theta_0)\frac{\rho_{V,sple}(\theta_0)}{\rho_{V,p-std}(\theta_0)}. \quad (1)$$

$G_{p-std}(\theta_0)$ is the specular gloss of a primary standard. $\rho_{V,sple}(\theta_0)$ and $\rho_{V,p-std}(\theta_0)$ are respectively the specular luminous reflectance of the sample and the specular luminous reflectance of the primary standard.

Definition of the specular luminous reflectance

Let's now define the term "specular luminous reflectance". Let's consider a light source with a spectral power density $\varphi(\lambda)$ at the wavelength λ measured in Watts (W/nm). The luminous flux in lumen (lm) related to $\Phi(\lambda)$ is defined by:

$$\Phi_V = K_M \int_\lambda \varphi(\lambda) V_\lambda(\lambda) d\lambda, \quad (2)$$

where $K_M = 683$ lm/W is the maximum spectral luminous efficacy for photopic vision and $V_\lambda(\lambda)$ is the Commission Internationale de l'Eclairage (CIE) 1924 photopic luminosity function. The specular luminous reflectance $\rho_V(\theta_0)$ of a surface is defined by the ratio:

$$\rho_V(\theta_0) = \frac{\Phi_{V,r}(\theta_0)}{\Phi_{V,i}}. \quad (3)$$

Charriere, Andree; Nadal, Maria; Zarobila, Clarence.
"Comparison of specular gloss values from a spectrally resolved
five-axis goniometer and a reference goniophotometer."
Paper presented at Material Appearance, Burlingame, CA. December 29, 2016 - January 2, 2017.

$\Phi_{V,r}(\theta_0)$ is the luminous flux reflected from the surface integrated over all incidence and reflection directions. A direction is defined by two angles θ and ϕ. θ and ϕ are respectively the polar and azimuthal angles in a spherical coordinate system with a zenith direction merged with the normal to the sample surface. Incidence directions are denoted with the subscript i and observation directions with the subscript r. We have then:

$$\Phi_{V,r}(\theta_0) = K_M \int_S \iint_{\theta_i,\phi_i} \iint_{\theta_r,\phi_r} \int_\lambda L_i(\theta_i,\phi_i,\lambda) BRDF(\theta_i,\phi_i,\theta_r,\phi_r,\lambda) V_\lambda(\lambda) \cos(\theta_i)\sin(\theta_i)\cos(\theta_r)\sin(\theta_r) d\lambda d\theta_i d\phi_i d\theta_r d\phi_r dS, \quad (4)$$

where $BRDF(\theta_i,\phi_i,\theta_r,\phi_r,\lambda)$ is the spectral BRDF of the surface and $L_i(\theta_i,\phi_i,\lambda)$ is the spectral radiance of the light illuminating the surface. S is the illuminated area of the surface. The dependency in θ_0 is not explicit in the right part of equation 4 but affects $L_i(\theta_i,\phi_i,\lambda)$, the domain of integration of the angles (θ_r,ϕ_r) and the surface S. The specular luminous reflectance is indeed measured in a specular geometry. $L_i(\theta_i,\phi_i,\lambda)$ will thus be a peak-shape function centered around the direction θ_0 from the normal of the sample surface. The illuminated surface S will be an elliptical surface with its major axis proportional to $\frac{1}{\cos(\theta_0)}$. The domain of integration of the angles (θ_r,ϕ_r) will be centered around the direction of the specular reflection on the sample, that is in a direction symmetrical to the incident light direction relatively to the sample surface normal.

For a perfectly flat material with an homogeneous refractive index $n(\lambda)$, the BRDF simplifies to [7]:

$$BRDF(\theta_i,\phi_i,\theta_r,\phi_r,\lambda) = \frac{\rho_{FR}(\theta_i,n(\lambda))}{\cos(\theta_r)\sin(\theta_r)} \delta(\theta_i-\theta_r)\delta(\phi_i-\phi_r\pm\pi), \quad (5)$$

where $\rho_{FR}(\theta_i,n(\lambda))$ is the Fresnel reflection coefficient for an incidence angle θ_i and a refractive index $n(\lambda)$. Gloss values are ideally measured with non-polarized light, so the Fresnel reflection coefficient to be considered here is for non-polarized light. $x \to \delta(x)$ is the Dirac delta function. In that case, the luminous reflected flux by the surface becomes:

$$\Phi_{V,r}(\theta_0) = K_M \iiint\iint_{S,\theta_i,\phi_i,\lambda} L_i(\theta_i,\phi_i,\lambda)\rho_{FR}(\theta_i,n(\lambda))V_\lambda(\lambda)\cos(\theta_i)\sin(\theta_i) d\lambda d\theta_i d\phi_i dS. \quad (6)$$

$\Phi_{V,i}$ is the luminous flux incident on the surface:

$$\Phi_{V,i} = K_M \int_\lambda \varphi_i(\lambda) V_\lambda(\lambda) d\lambda, \quad (7)$$

with $\varphi_i(\lambda)$ being the spectral power density of the light incident on the surface. Note that we have the following relationship:

$$\iiint_{S,\theta_i,\phi_i} L_i(\theta_i,\phi_i,\lambda)\cos(\theta_i)\sin(\theta_i) d\theta_i d\phi_i dS = \varphi_i(\lambda). \quad (8)$$

ASTM D523 precisely specifies the geometries through which the luminous reflectance has to be measured. The angular field apertures for the source and the receiver in the incidence plane (respectively Θ_i^{IP} and Θ_r^{IP}) and perpendicular to the incidence plane (resp. Θ_i^{PIP} and Θ_r^{PIP}) are defined, according to figure 1, in a plane which is conjugated with the "real" source field aperture through the source and receiver lenses. Note that the definition presented in figure 1 is valid only for so called "parallel beam glossmeters", that is glossmeters where the beam incident on the sample would be perfectly collimated in case of a point light source. The values of the angles Θ_i^{IP}, Θ_i^{PIP}, Θ_r^{IP} and Θ_r^{PIP} for the three standards incidence angles 20°, 60° and 85° and the corresponding tolerances are given in table 1. The tolerance on the angular values 20°, 60° and 85° is 0.1°.

Table 1. ASTM D523 source image and receiver angular apertures specifications and tolerances.

Apertures	Parallel to the plane of incidence [°]	Perpendicular to the plane of incidence [°]
	$2\Theta_i^{IP}$	$2\Theta_i^{PIP}$
Source image	0.75 ± 0.25	2.5 ± 0.5
	$2\Theta_r^{IP}$	$2\Theta_r^{PIP}$
20° receiver	1.8 ± 0.05	3.6 ± 0.1
60° receiver	4.4 ± 0.1	11.7 ± 0.2
85° receiver	4 ± 0.3	6 ± 0.3

ASTM D523 specifies also that "the obtained results should not differ significantly from those obtained with a source-filter combination that is spectrally corrected to yield CIE luminous efficiency with CIE source C". That is, by referring to our previous notations, we should obtain the same results as if $\varphi_i(\lambda)$ were proportional to the spectral power density $C(\lambda)$ of the CIE illuminant C.

Definition of the primary standard specular gloss value

Gloss values are calculated relatively to a reference standards. The theoretical reference standard for gloss measurements is specified to be a highly polished plane black glass with an index of refraction at the wavelength of the sodium D line ($\lambda_D = 589.3$ nm) equal to $n_{th-std}(\lambda_D) = 1.567$. The gloss value for this theoretical standard is set to 100 for the three standard specular geometries 20°, 60°and 85°. Primary standards are used since these specifications are not found in real materials. The gloss value $G_{p-std}(\theta_0)$ of the primary standard illuminated with light around the direction θ_0 from the normal of its surface is defined by the following equation:

$$G_{p-std}(\theta_0) = 100 \frac{\rho_{FR}(\theta_0, n_{p-std}(\lambda_D))}{\rho_{FR}(\theta_0, n_{th-std}(\lambda_D))}, \quad (9)$$

where $n_{th-std}(\lambda_D)$ is the refractive index of the theoretical standard at the wavelength λ_D.

Note that an alternative definition for $G_{p-std}(\theta_0)$ can be used, by replacing the Fresnel reflection coefficient $\rho_{FR}(\theta_0, n_{p-std}(\lambda_D))$ by the measured specular luminous reflectance of the primary standard.

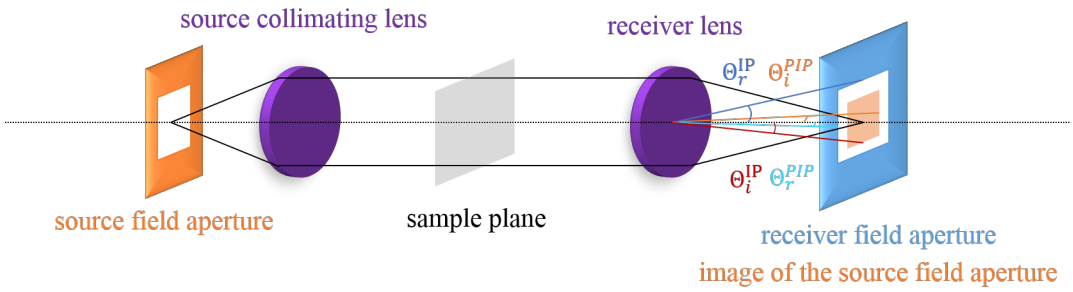

Figure 1. *Diagram of the optical system of a parallel beam glossmeter showing the definitions of the angular source (θ_s) and receiver (θ_r) field apertures.*

Proposed Goniometer modifications

A detailed description of the original optical system for the Five-Axis Goniometer is given in reference [5]. Figure 2 shows the proposed optical layout on the Five Axis Goniometer in order to be able to measure specular gloss according to ASTM D523. A high power broadband Laser Driven Light Source (LDLS) was chosen as the illuminating source making it possible to measure low gloss samples. Broadband white light is generated by a continuous laser focused in a xenon plasma. The white light is then collected through an elliptical reflector. This reflector has a hole in order to allow the continuous laser to reach the plasma. Consequently the cross-section of the beam generated by the LDLS source has a doughnut shape in the far field, even after a multimode 910 μm fiber. A set of two microlens arrays in imaging configuration is added on the beam path in order to improve the homogeneity of the beam cross-section.

The conjugation ratio for the source aperture is equal to 1 as it is imaged in the receiver field aperture plane through two 150 mm focal length lenses in $f-\infty-f$ configuration. In order to follow ASTM D523 angular specifications (see table 1), the source and receiver apertures are rectangular, with angular dimensions specified in table 2.

Table 2. Source and receiver apertures dimensions. Each dimension is equal to the focal length of the receiver lens (150 mm) multiplied by the tangent of the angular value specified in table 1.

Apertures	Parallel to the plane of incidence	Perpendicular to the plane of incidence
Source	1.96 mm	6.55 mm
20° receiver	4.71 mm	9.43 mm
60° receiver	11.53 mm	30.74 mm
85° receiver	10.48 mm	15.72 mm

A beam-splitter and a fiber-coupled spectrometer will be added in the beam path to correct for power fluctuations of the illuminating beam. The beam reflected by the sample will go through the receiver aperture into an integrating sphere. A fiber used at one port of the integrating sphere brings the beam into a spectrometer.

Experimental computation of the gloss value

The gloss value is measured by simultaneously acquiring the monitor beam and the spectrum given by the receiver spectrometer for both the test sample and the primary standard. Let's denote respectively by $\mathscr{S}_m^{sple}(\lambda)$ and $\mathscr{S}_r^{sple}(\lambda)$ the spectra given by the monitor and the receiver spectrometers when measuring the sample and by $\mathscr{S}_m^{p-std}(\lambda)$ and $\mathscr{S}_r^{p-std}(\lambda)$ the spectra given by the monitor and the receiver spectrometers when measuring the primary standard.

Therefore, for the monitor signal:

$$\mathscr{S}_m^x(\lambda) = \mathscr{R}_{msp}(\lambda)T_{mf}(\lambda)T_{L60}(\lambda)R_{GP}(\lambda)\phi_i^x(\lambda), \qquad (10)$$

where x superscript is either $sple$ or $p-std$. $\mathscr{R}_{msp}(\lambda)$ is the spectral responsivity of the monitor spectrometer in counts/W, $T_{mf}(\lambda)$ is the spectral transmittance of the fiber bringing the light into the monitor spectrometer, $T_{L60}(\lambda)$ is the spectral transmittance of the 60 mm focal lens achromat injecting the light into the monitor fiber and $R_{GP}(\lambda)$ is the spectral reflectance of the glass plate extracting a part of the beam incident on the sample into the monitor arm (see figure 2). $\phi_i^x(\lambda)$ is the spectral power density of the light incident either on the sample or on the primary standard. Note that without any temporal fluctuations of the light source, we should have $\phi_i^{sple}(\lambda) = \phi_i^{p-std}(\lambda)$ and consequently $\mathscr{S}_m^{sple}(\lambda) = \mathscr{S}_m^{p-std}(\lambda)$. Equation 10 neither takes into account potential non-linearity of the spectrometer responsivity nor potential wavelength shift due to non-perfect calibration of the spectrometer.

For the receiver spectrum of the test sample, we have:

$$\mathscr{S}_r^{sple}(\lambda) = \mathscr{R}_{rsp}(\lambda)T_{rf}(\lambda)\mathscr{R}_{is}(\lambda)T_{L150}(\lambda)T_{GP}(\lambda)\int_S\iiiint_{\theta_i,\phi_i,\theta_r,\phi_r} L_i^{sple}(\theta_i,\phi_i,\lambda)BRDF^{sple}(\theta_i,\phi_i,\theta_r,\phi_r,\lambda)\cos(\theta_i)\sin(\theta_i)\cos(\theta_r)\sin(\theta_r)d\theta_i d\phi_i d\theta_r d\phi_r dS. \qquad (11)$$

$\mathscr{R}_{rsp}(\lambda)$ is the spectral responsivity of the receiver spectrometer in counts/W, $T_{rf}(\lambda)$ is the spectral transmittance of the fiber bringing the light into the receiver spectrometer, $\mathscr{R}_{is}(\lambda)$ is the spectral responsivity of the integrating sphere (this is a global factor including all geometrical considerations related to the integrating sphere and the injection of the light into the receiver fiber), $T_{L150}(\lambda)$ is the spectral transmittance of the 150 mm focal lens achromat bringing the light reflected by the sample into the

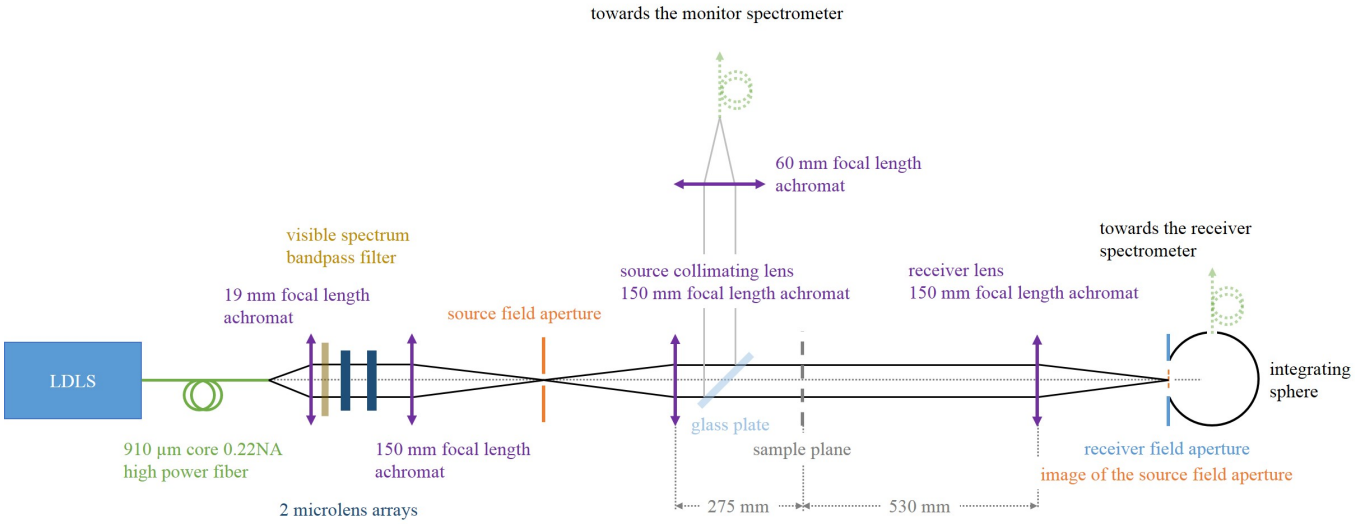

Figure 2. *Diagram of the proposed optical system to measure gloss on the Five-Axis Goniometer. Note that distances are not to scale on the diagram. The distance between the two lenses surrounding the two microlens arrays is about 15 mm and the distance between the two microlens arrays is equal to the focal lens of the microlenses (5.1 mm).*

integrating sphere and $T_{GP}(\lambda)$ is the spectral transmittance of the glass plate. All other notations are the same as in equation 4.

The equation for the receiver spectrum of the primary standard is more simple than for the test sample. The primary standard used at NIST is an optical quality barium crown glass BaK50 with an index of refraction at the wavelength λ_D equal to $n_{p-std}(\lambda_D) = 1.5677$ [6]. The front surface of the primary standard were polished to a roughness of 0.6 nm. For this reason, the primary standard can be considered as a perfectly flat sample and it's BRDF can be simplified according to equation 5. We thus have:

$$\mathscr{S}_r^{p-std}(\lambda) = \mathscr{R}_{rsp}(\lambda)T_{rf}(\lambda)\mathscr{R}_{is}(\lambda)T_{L150}(\lambda)T_{GP}(\lambda)\int_S\iint_{\theta_i,\phi_i} L_i^{p-std}(\theta_i,\phi_i,\lambda)\rho_{FR}(\theta_i,n_{p-std}(\lambda))\cos(\theta_i)\sin(\theta_i)d\theta_i d\phi_i dS. \quad (12)$$

A direct measurement of both monitor and receiver spectra with the incident beam striking directly on the receiver arm (that is without any interaction with a sample) is necessary to get rid of the spectral responsivities of the various optical elements (lenses, glass plate, fibers, spectrometers, integrating sphere...) present on the path of the beam either in the monitor arm or in the receiver arm. Let's denote respectively by $\mathscr{S}_m^0(\lambda)$ and $\mathscr{S}_r^0(\lambda)$ the spectra given by the monitor and the receiver spectrometers when the incident beam is striking directly the receiver arm. We have:

$$\begin{cases} \mathscr{S}_m^0(\lambda) &= \mathscr{R}_{msp}(\lambda)T_{mf}(\lambda)T_{L60}(\lambda)R_{GP}(\lambda)\phi_i^0(\lambda) \\ \mathscr{S}_r^0(\lambda) &= \mathscr{R}_{rsp}(\lambda)T_{rf}(\lambda)\mathscr{R}_{is}(\lambda)T_{L150}(\lambda)T_{GP}(\lambda)\phi_i^0(\lambda) \end{cases}. \quad (13)$$

where $\phi_i^0(\lambda)$ is the Power Spectral Density of the light incident on the sample plane. Note that as the monitor and the receiver signals are acquired at the same time, computing the ratio $\mathscr{Q}_0(\lambda) = \frac{\mathscr{S}_r^0(\lambda)}{\mathscr{S}_m^0(\lambda)}$ allows to get rid of the spectral responsivity of the various elements present on the beam paths excluding all source temporal fluctuations.

To compute the gloss value of the sample from the experimentally measured quantities, we first compute, as a function of wavelength, the following quantities:

$$\begin{cases} \dfrac{\mathscr{Q}_{sple}(\lambda)}{\mathscr{Q}_0(\lambda)} &= \dfrac{\mathscr{S}_r^{sple}(\lambda)}{\mathscr{S}_m^{sple}(\lambda)}\dfrac{1}{\mathscr{Q}_0(\lambda)} \\ \dfrac{\mathscr{Q}_{p-std}(\lambda)}{\mathscr{Q}_0(\lambda)} &= \dfrac{\mathscr{S}_r^{p-std}(\lambda)}{\mathscr{S}_m^{p-std}(\lambda)}\dfrac{1}{\mathscr{Q}_0(\lambda)} \end{cases}. \quad (14)$$

The choice has been made on our optical design neither to try to generate a spectral power density of the light incident on the sample close to the CIE illuminant C nor to simulate a $V_\lambda(\lambda)$ responsivity for the receiver. Custom made filters are quite expensive and don't allow any flexibility on the experimental setup. To determine the gloss value of the sample, the specular luminous reflectances of the sample and the primary standard are computed from the experimentally measured quantities. Computing the ratios $\mathscr{Q}_{sple}$ and $\mathscr{Q}_{p-std}$ allows to get rid of temporal fluctuations of the source between the measurements of the sample and the primary standard. These normalized quantities are independent of the spectral power density of the illuminating source. While neglecting all chromatic aberrations of the optical elements, angular and spectral variations of the radiance of the incident light can also be considered as uncoupled. We can thus write $L_i^x(\theta_i,\phi_i,\lambda) = \tilde{L}_i(\theta_i,\phi_i)l^x(\lambda)$, where $l^x(\lambda)$ includes spectral variations as well as potential temporal variations of the source. Then equation 14 becomes:

$$\begin{cases} \dfrac{\mathscr{Q}_{sple}(\lambda)}{\mathscr{Q}_0(\lambda)} & = & \dfrac{\int_S \iiiint_{\theta_i,\phi_i,\theta_r,\phi_r} \tilde{L}_i(\theta_i,\phi_i) BRDF^{sple}(\theta_i,\phi_i,\theta_r,\phi_r,\lambda)\cos(\theta_i)\sin(\theta_i)\cos(\theta_r)\sin(\theta_r)d\theta_i d\phi_i d\theta_r d\phi_r dS}{\int_S \iint_{\theta_i,\phi_i} \tilde{L}_i(\theta_i,\phi_i)\cos(\theta_i)\sin(\theta_i)d\theta_i d\phi_i dS} \\ \dfrac{\mathscr{Q}_{p-std}(\lambda)}{\mathscr{Q}_0(\lambda)} & = & \dfrac{\int_S \iint_{\theta_i,\phi_i} \tilde{L}_i(\theta_i,\phi_i)\rho_{FR}(\theta_i,n_{p-std}(\lambda))\cos(\theta_i)\sin(\theta_i)d\theta_i d\phi_i dS}{\int_S \iint_{\theta_i,\phi_i} \tilde{L}_i(\theta_i,\phi_i)\cos(\theta_i)\sin(\theta_i)d\theta_i d\phi_i dS} \end{cases} . \quad (15)$$

The gloss value of the sample is then computed by the following formula:

$$G^{exp}_{sple}(\theta_0) = 100\frac{\rho_{FR}(\theta_0,n_{p-std}(\lambda_D))}{\rho_{FR}(\theta_0,n_{th-std}(\lambda_D))}\frac{\sum_{\lambda_i} V_\lambda(\lambda_i)C(\lambda_i)\frac{\mathscr{Q}_{sple}(\lambda_i)}{\mathscr{Q}_0(\lambda_i)}}{\sum_{\lambda_i} V_\lambda(\lambda_i)C(\lambda_i)\frac{\mathscr{Q}_{p-std}(\lambda_i)}{\mathscr{Q}_0(\lambda_i)}}, \quad (16)$$

The wavelengths λ_i range is from 380 nm to 780 nm by increments of either 5 nm or 10 nm.

Comparison between BRDF and gloss measurements

The BRDFs of two black glass samples with different gloss levels have been measured with the Five-Axis Goniometer for the visible spectrum (380 nm to 780 nm). Note that the BRDF measurements were made with the goniometer's original optical system [5], not the proposed modification shown in figure 2. These samples are denoted NIST-SG#6 and NIST-SG#7. The NIST BaK50 gloss primary standard has been also measured with the Five-Axis Goniometer to calibrate the response of the goniometer. The gloss values of these samples, measured with the Reference Goniophotometer for Specular Gloss Calibration are presented in table 3. Note that the uncertainties for the gloss measurements using the Reference Goniophotometer are in the order of 0.8% to 1.5% and the uncertainties for the gloss measurements using the Five-Axis Goniometer are in the order of 2% to 3%.

Table 3. Gloss values measured with the Reference Goniophotometer for Specular Gloss Calibration of the black glass samples NIST-SG#6 and NIST-SG#7 and of the NIST BaK50 gloss primary standard at incidence angles of 20°and 60°.

Sample name	Gloss value for incidence angle 20°	Gloss value for incidence angle 60°
NIST-SG#6	70.8	91.2
NIST-SG#7	8.9	48.2
BaK50	100.8	100.6

For the work with the Five-Axis Goniometer, we will first focus on the wavelength of 500 nm. Figure 3 represents BRDF measurements in the incidence plane at 20°and 60°incidence angles for the two black glass samples NIST-SG#6 and NIST-SG#7 as well as for the BaK50 NIST gloss primary standard. Both the Full Width at Half Maxiumum (FWHM) and the maximum value of the BRDF are linked to the gloss value of the sample (see table 4). As observed by Leloup et al. in reference [8], the width of the BRDF doesn't depend much on the incidence angle, whereas, in accordance with the Fresnel equations giving the reflectance factor of a perfectly flat and homogeneous surface, the maximum value of the BRDF increases with the incidence angle.

Table 4. BRDF maximum and FWHM for the samples NIST-SG#6, NIST-SG#7 and the BaK50 NIST gloss primary standard at incidence angles of 20°and 60°.

Sample name	BRDF maximum for incidence angle 20°	FWHM of BRDF peak for incidence angle 20°	BRDF maximum for incidence angle 60°	FWHM of BRDF peak for incidence angle 60°
NIST-SG#6	22.9 sr^{-1}	2.7°	102.3 sr^{-1}	2.7°
NIST-SG#7	2.4 sr^{-1}	6.8°	23.1 sr^{-1}	5°
BaK50	30.8 sr^{-1}	2.6°	125.7 sr^{-1}	2.5°

The BaK50 primary standard has a highly polished surface and the shape of the curve given by the goniometer is not related to the sample surface properties but characterizes the response of the goniometer. Experimentally, the BRDF is computed on the Five-Axis Goniometer by the following formula [5]:

$$BRDF(\theta_i,\phi_i,\theta_r,\phi_r,\lambda) = \frac{\Phi_R(\theta_i,\phi_i,\theta_r,\phi_r,\lambda)}{\Phi_i(\lambda)\cos(\theta_r)\Omega}, \quad (17)$$

where $\Phi_R(\theta_i,\phi_i,\theta_r,\phi_r,\lambda)$ is the flux reflected by the sample collected by the receiver. $\Phi_i(\lambda)$ is the flux incident on the sample, measured when the incident beam is striking directly the receiver. Ω is the receiver collection solid angle. The Fresnel equations give us the values of the ratio $\frac{\Phi_R(\theta_i,\phi_i,\theta_r=\theta_i,\phi_r=\phi_i+180°,\lambda)}{\Phi_i(\lambda)}$ from the refractive index values of the sample. Thus, in case when the shape of the experimental BRDF is limited by the goniometer response, multiplying the maximum value of the BRDF by $\cos(\theta_r)\Omega$ allows us to retrieve the Fresnel reflectance factor. The refractive index values of the BaK50 primary standard are given in reference [6]. For this sample, the values of the Fresnel reflectance factor and the product of the maximum value of the measured BRDF by $\cos(\theta_r)\Omega$ can thus be compared (see table 5). Note that the goniometer source is supposed to be perfectly non-polarized and the Fresnel reflectance factors are thus computed for non-polarized light.

As observed on figure 3 and in table 4, the FWHM value of the BRDF of the NIST-SG#6 sample is very close to that of the BaK50 standard, whereas the FWHM value of the BRDF of the NIST-SG#7 sample is about twice as higher. The shape of the NIST-SG#6 BRDF is thus mainly related to the goniometer response, whereas the shape of the NIST-SG#7 BRDF is clearly influenced by the surface properties of the sample. In the case

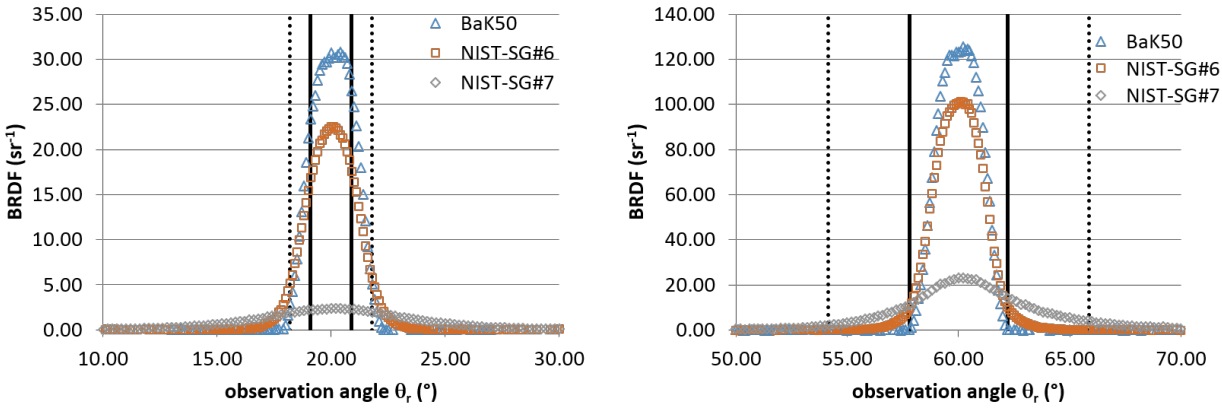

Figure 3. *BRDF measurements in the incidence plane at 20° (left) and 60° (right) incidence angles of two black glass samples with different gloss levels for a wavelength of 500 nm. The red curves represent the BRDFs of the sample NIST-SG#6 and the gray curves the BRDFs of the sample NIST-SG#7. The blue curves represent the measurements of the BaK50 NIST gloss primary standard. The black solid vertical lines delimit the ASTM D523 angular receiver aperture specifications in the incidence plane for 20° and 60° geometries. The black dashed vertical lines delimit the ASTM D523 angular receiver aperture specifications perpendicular to the incidence plane for 20° and 60° geometries.*

Table 5. Products of the maximum value of the measured BRDFs by $\cos(\theta_r)\Omega$ at incidence angles of 20°and 60°for the samples NIST-SG#6, NIST-SG#7 and the BaK50 NIST gloss primary standard. Are also indicated the non-polarized Fresnel reflectance factors computed from the BaK50 refractive index values.

Sample name	$BRDF_{max}\cos(\theta_r)\Omega$ for incidence angle 20°	$BRDF_{max}\cos(\theta_r)\Omega$ for incidence angle 60°
NIST-SG#6	0.0381	0.0924
NIST-SG#7	0.0021	0.0385
BaK50	0.0513	0.1135
BaK50 Fresnel	0.0500	0.1012

where the shape of the measured BRDF doesn't characterize the surface properties of the sample, the first equation of the equation array 15 has to be replaced by:

$$\frac{\mathcal{Q}_{p-std}(\lambda)}{\mathcal{Q}_0(\lambda)} = \frac{\int_S \iint_{\theta_i,\phi_i} \tilde{L}_i(\theta_i,\phi_i)\rho_{FR}(\theta_i,n_{sple}(\lambda))\cos(\theta_i)\sin(\theta_i)d\theta_i d\phi_i dS}{\int_S \iint_{\theta_i,\phi_i} \tilde{L}_i(\theta_i,\phi_i)\cos(\theta_i)\sin(\theta_i)d\theta_i d\phi_i dS}, \tag{18}$$

where $n_{sple}(\lambda)$ is the refractive index of the sample at the wavelength λ. By neglecting also the variations of the Fresnel reflectance factor of both the sample and the primary standard with θ_i, the equation 16 can be then approximated by:

$$G^{exp}_{sple}(\theta_0) = 100\frac{\rho_{FR}(\theta_0,n_{p-std}(\lambda_D))}{\rho_{FR}(\theta_0,n_{th-std}(\lambda_D))}\frac{\sum_{\lambda_i} V_\lambda(\lambda_i)C(\lambda_i)\rho_{FR}(\theta_0,n_{sple}(\lambda_i))}{\sum_{\lambda_i} V_\lambda(\lambda_i)C(\lambda_i)\rho_{FR}(\theta_0,n_{p-std}(\lambda_i))}. \tag{19}$$

Let first assume that, for both NIST-SG#6 and NIST-SG#7 samples, the previous approximation is valid and that the product of the maximum value of the BRDF by $\cos(\theta_r)\Omega$ gives us the Fresnel reflectance factor of the samples. We thus calculate the gloss value of these samples according to equation 19. The results are presented in table 6. For NIST-SG#6 sample, the calculated gloss values compared well with the measured values listed in table 3 particularly for the incidence angle of 60°. For NIST-SG#7 sample, we observe that the calculated 20°gloss value is in good agreement with the value measured with the Reference Goniophotometer for Specular Gloss Calibration, but not the calculated value for the 60°geometry. In the case where the shape of the BRDF is clearly limited by the angular resolution of the goniometer, gloss values computed from the maximum of the BRDF are in good agreement with the values measured with the Reference Goniophotometer for Specular Gloss Calibration. For the NIST-SG#7 sample a good agreement is obtained at 20°that is in the case where the ASTM D523 angular receiver specifications include an area where the BRDF is nearly equal to is maximum value (see figure 3).

Table 6. Gloss values of NIST-SG#6 and NIST-SG#7 samples computed according to equation 19 assuming the maximum of the measured BRDF is directly related to the Fresnel reflectance factor of the sample.

Sample name	Gloss value computed from BRDF maximum for incidence angle 20°	Gloss value computed from BRDF maximum for incidence angle 60°
NIST-SG#6	75.6	90.9
NIST-SG#7	8.3	22.5

To compute properly the gloss value of the NIST-SG#7 sample from its BRDF, equations 15 and 16 need to be used. These equations require to know the variations of the BRDF with the five variables $\theta_i, \phi_i, \theta_r, \phi_r$ and λ. We will neglect the variations of the BRDF with θ_i and ϕ_i. First BRDF measurements have been done only in the incidence plane. To compute the integration of the BRDF over the geometrical extent defined by the ASTM D523 receiver aperture specifications, the out of plane values of the BRDF have be numerically computed assuming a rotational symmetry

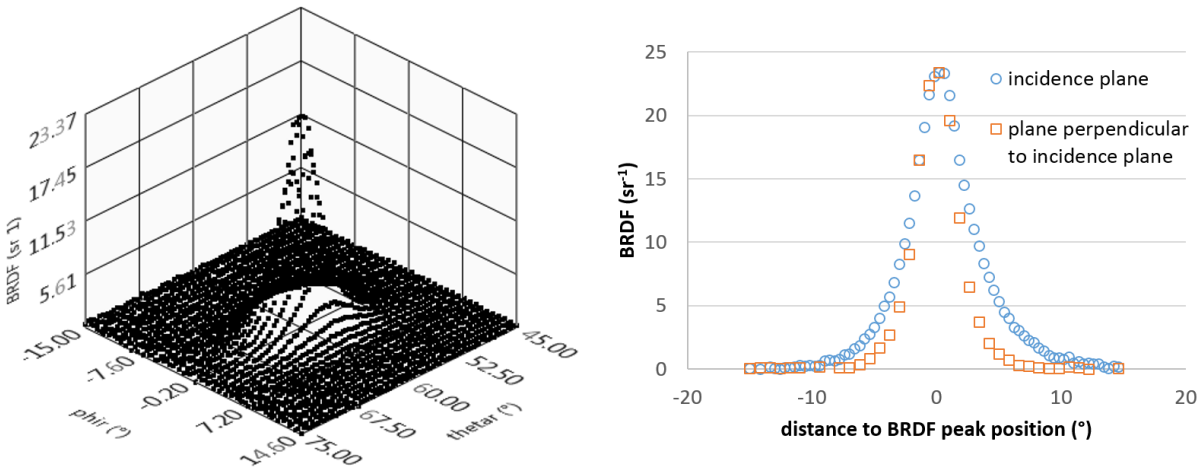

Figure 4. *Three dimensional measurement of the BRDF of the NIST-SG#7 sample (left) for an incidence angle of 60°. Comparison between the BRDF profiles of the NIST-SG#7 sample extracted from the three dimensional measurement in the incidence plane and perpendicular to the incidence plane (right).*

of the BRDF. Note that the integration domain is a rectangle in the (θ_r, ϕ_r) plane with side lengths defined in table 1. Table 7 shows the gloss values computed this way for both NIST-SG#6 and NIST-SG#7 samples. We observe that for the NIST-SG#6 sample at the incidence angle of 60°the gloss value is still close to the value measured with the Reference Goniophotometer for Specular Gloss Calibration (see table 3) whereas the gloss value for the incidence angle of 20°is not the expected value. For the NIST-SG#7 sample the gloss value at the incidence angle of 20°is also not the expected value. Nevertheless the value at 60°is closer to the expected value than the value computed from the BRDF maximum value (see table 6).

Table 7. Gloss values of NIST-SG#6 and NIST-SG#7 samples computed according to equations 15 and 16 assuming the shape of the measured BRDF characterizes the surface properties of the sample.

Sample name	Gloss value computed from BRDF integration for incidence angle 20°	Gloss value computed from BRDF integration for incidence angle 60°
NIST-SG#6	18.1	89.0
NIST-SG#7	3.0	61.8

The gloss values listed on the table 7 have been computed by assuming a rotational symmetry of the BRDF. To study the influence of this assumption on the gloss value a three dimensional measurement of the BRDF of the NIST-SG#7 sample for an incidence angle of 60°have been performed (see figure 4). We observe that the profiles of the BRDF in the incidence plane and perpendicular to the incidence plane are slightly different. The gloss value computed from this three dimensional BRDF measurement is closer to the value measured with the Reference Goniophotometer for Specular Gloss Calibration than the value computed from in plane BRDF measurements and assuming a rotational symmetry of the BRDF (see tables 8 and 7).

Table 8. Comparison between the gloss value of NIST-SG#7 sample at an incidence angle of 60°computed according to equations 15 and 16 from a three dimensional BRDF measurement and its gloss value at the same incidence angle measured with the Reference Goniophotometer for Specular Gloss Calibration.

Gloss value computed from 3D BRDF measurement	Gloss value measured with the Reference Goniophotometer for Specular Gloss Calibration
53.3	48.2

Conclusion and perspectives

The preliminary results presented in this paper show that a good agreement can be obtained between gloss measurements performed on a device dedicated to gloss calibration and following ASTM D523 specifications (the Reference Goniophotometer for Specular Gloss Calibration) and BRDF measurements, particularly for high (around 90) or low (around 10) gloss values and in the case where the maximum value of BRDF is used to evaluate the Fresnel reflectance factor of the sample. The way to compute the gloss value from the BRDF is highly dependent on the relationship between the width of the angular device response and the angular response of the studied material. In the case where the shape of the measured BRDF if limited by the device response, the maximum value of the BRDF is linked to the gloss value of the sample. On the contrary, when the shape of the measured BRDF is linked to the surface properties of the material, an integration of the BRDF over the receiver geometrical extent defined by ASTM D523 need to be performed. In this case, computing the gloss value from a three dimensional BRDF measurement seems to give more accurate results. These results need to be confirmed by additional measurements on samples describing a more extended and detailed scale of gloss values. Intermediate cases where the shape of the BRDF is linked partially to the device response and partially to the sample response will certainly need to decorrelate both influences before computing the gloss value.

Charriere, Andree; Nadal, Maria; Zarobila, Clarence.
"Comparison of specular gloss values from a spectrally resolved
five-axis goniometer and a reference goniophotometer."
Paper presented at Material Appearance, Burlingame, CA. December 29, 2016 - January 2, 2017.

We have also proposed modifications to the existing Five-Axis Goniometer that should enable its use as a direct replacement for the Goniometer for Specular Gloss Calibration. In the future, we plan to test these modifications and hopefully demonstrate the suitability of the modified instrument for providing gloss calibrations.

References

[1] W. Budde, "The Calibration of Gloss Reference Standards," *Metrologia*, vol. 16, pp. 89–93, 1980.

[2] "ASTM D523-14 Standard Test Method for Specular Gloss," *ASTM International*, 2014.

[3] F. B. Leloup, G. Obein, M. R. Pointer, and P. Hanselaer, "Toward the soft metrology of surface gloss: A review," *Color Research and Application*, vol. 39, no. 6, pp. 559–570, 2014.

[4] F. Vienot and G. Obein, "Is gloss recognized as a surface property?," in *Proceedings of MS 2004, 1st International Workshop on Materials and Sensations*, pp. 77–82, 2004.

[5] G. Obein, R. Bousquet, and M. E. Nadal, "New NIST reference goniospectrometer," in *SPIE Proceedings*, vol. 5880, International Society for Optics and Photonics, aug 2005.

[6] M. E. Nadal, E. A. Early, and E. A. Thompson, "Specular Gloss," *NIST Special Publication*, vol. SP250-70, 2006.

[7] T. A. Germer, J. C. Zwinkels, and B. K. Tsai, eds., *Spectrophotometry: Accurate Measurement of Optical Properties of Materials*. Academic Press, 2014.

[8] F. Leloup, P. . Hanselaer, J. Versluys, and S. Forment, "BRDF AND GLOSS MEASUREMENTS," in *Proceedings of the CIE expert symposium on visual appearance, CIE (Commission International de l'Eclairage)*, 2006.

Author Biography

Renee Charriere has completed a PhD in Optics and Quantum Mechanics in 2011 in the French Aerospace Lab (Office National dEtudes et de Recherches Arospatiales) and Paris VI University. As postdoctoral fellow she worked on the optical characterization and modeling of nanostructured surfaces with complex visual appearance. She is now assistant professor at the French Laboratory Georges Friedel in Saint-Etienne and is currently guest researcher at National Institute of Standards and Technology in USA.

Charriere, Andree; Nadal, Maria; Zarobila, Clarence.
"Comparison of specular gloss values from a spectrally resolved
five-axis goniometer and a reference goniophotometer."
Paper presented at Material Appearance, Burlingame, CA. December 29, 2016 - January 2, 2017.